Applied GIS

ISSN: 1832-5505
Vol-7 Issue-01 FEB 2019

Enhancement of Voltage Stability and Power Quality for Ship board Systems with PR based SVPWM Controller

K.SREENIVASULU, ASSISTANT PROFESSOR, chitrasreenu44@gmail.com
C.RAMESH BABU, ASSISTANT PROFESSOR, ramesh.babu224@gmail.com
D.SHEKSHA VALI, ASSISTANT PROFESSOR, shaiksha456@gmail.com
Department of Electrical & Electronics Engineering, Sri Venkateswara Institute of Technology,
N.H 44,Hampapuram, Rapthadu, Anantapuramu, Andhra Pradesh 515722D

Abstract: The expansion of power electronics technology has recently been drawn to shipboard power systems (SPSs). But stabilising the harmonics owing to nonlinear load and component qualities is the primary focus of SPSs.In addition, a voltage drop might be caused by the rapidly pulsing loads pulling enormous currents in a very short period of time. The voltage will fall when it surpasses its limit, which might cause the spacecraft to shut down. To overcome these challenges, a hybrid active power filter (HAPF) and a fixed capacitor-thyristor controlled reactor (FC-TCR) with proportional resonant-based state vector pulse width modulation (PR-SVPWM) technique were integrated.In the MATLAB/Simulink environment, the suggested system has been constructed. The proposed system has been tested in a number of different dynamic scenarios, and its performance has been monitored. The simulation results show that the suggested PR-based SVPWM outperforms the alternatives when it comes to harmonic reduction.

Keywords : dynamic power filter, shipboard, power systems, fixed capacitor, SVPWM

Introduction

There is a significant difference between the needs for power production and distribution on land and those for shipboard electrical systems. When designing power distribution systems for ships, electrical engineers must keep safety and efficiency in mind.Commercial ships, naval vessels, offshore floating platforms, and offshore support boats are all part of the shipboard power system, and this book covers all the key technologies and regulations for creating these systems.(1) and (2).Offshore floating platforms have been brought up a lot in the context of deep-water resource exploration in the last few years [3][4].Every step of designing and verifying a shipboard electrical system is laid out in this book.

covers the basics as well as specific electrical devices, offers design examples, and gives sufficient visuals to support its claims.
The ensuing measures to ensure the safety of the boat by reducing the likelihood of a power loss while at sea. Moreover, voltage flimsiness caused by steady-state loads could be an outcome of the controllability provided by force-electronic converters for propellers [5]. There are a few suggestions for symphonic moderation throughout the text. To compensate for a lack of receptive force, the latent force channels (PPFs) were often used to stifle the most powerful noises [6]. However, there are a few shortcomings that the PPFs have to deal with, the most significant of which being the reverberation risk and the set responding force pay. The catastrophic PPFs accident, which RMS Queen Mary II (QMII) oversaw, is most likely caused by the vaporisation of the PPFs, according to the examination's most

ISSN: 1832-5505
Vol-7 Issue-01 FEB 2019

significant probability [7]. By using APFs, the drawback of PPFs may be avoided [8, 9]. The substantial cost, however, limits their usefulness. An option to reduce the SAPF's cost was the HAPF [10]. One configuration of the HAPF with PPFs in conjunction with APFs reduces the converter's DC power rating by acting as a low pass filter for most background noise and a high pass filter for the main signal [11]. But shunt HAPFs can't fix voltage and current problems at the same time. Combination APFs (arrangement APFs and shunt APFs) and similar arrangements aren't a reliable alternative due to the higher cost.The APF dampens the sound and the TCR handles the receptive force in[12],[13]using FC-TCRimproves the overall compensator's efficiency. However, according to [14], productive voltage soundness is not the same as repaying the force factor (PF) towards solidarity. Voltage deficit, also known as voltage collapse, may be caused by either the inability to pay or excessive compensation for PF, as will be shown in this paper's section III. A shipwide blackout can occur if the latter is not addressed promptly.

1.0 Suggestedmethodmodelling

As shown in Figure 1 (a), the EPS that has been modelled is a simpler SPS. Every one of its two sections has the same components: two generators, two pulsed loads (propellers), two variable-speed drives (a HAPF) linked to the control panel, and two FC-TCR filters linked to the heavy lifting equipment.Figure 1(b) shows a simplified single-line version of Figure 1(a), which makes the modelling and the examination of the EPS.By representing the non-linear loads as linear loads plus current harmonic sources, the bottom schematic of Figure 1(b) aids the top one.

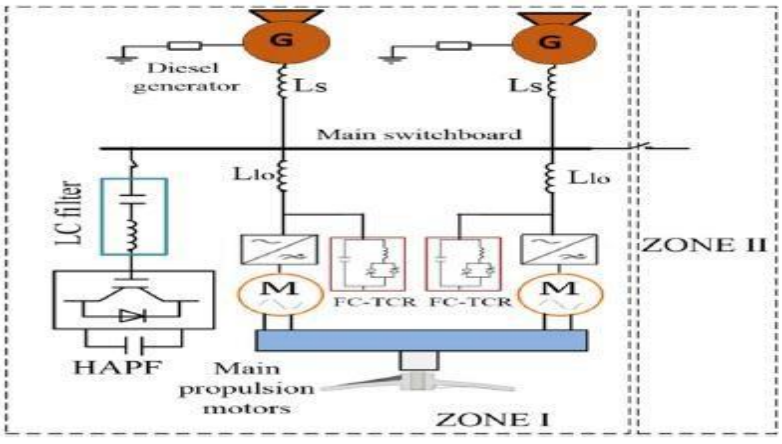

(a)

Applied GIS

ISSN: 1832-5505
Vol-7 Issue-01 FEB 2019

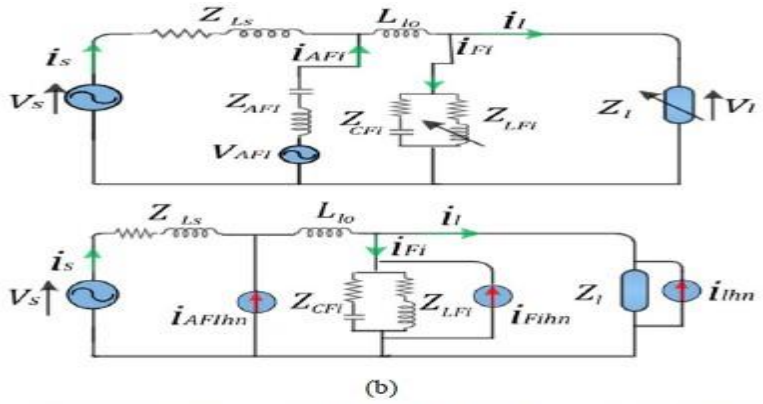

(b)

Fig. 1: single line diagram of the FC-TCR HAP connected to the EPS of a shipboard power system. *(a)* Schematic diagram of the ship power system including two generators, two propellers, and FC-TCR HAPF. *(b)* Simplified diagram of the EPS under investigation.

In addition, the HAPF might be included as a harmonic source in the voltage stability analysis since its job is to reduce harmonics.

A. The FC-TCR Compensator: Modelling and Control

Since the second propeller and FC-TCT are conceptually identical, we will focus on modelling only one of these components for the purpose of simplicity. Lo L's job is to dampen the power converters' distorted output when the speed varies. In addition, the FC-TCR may function as a low-pass filter due to its connection following lo L. The voltage distortion generated by the power converters is therefore reduced.In addition, the flow of the reactant power produced by the FC-TCR via lo L

findings in recouping the voltage losses brought on by the large loads, as will be seen in the results.Figure 2 (a) shows the FC-TCR's closed loop control mechanism. The voltage difference between the load and the reference voltage from the source (s V) is used to calculate the error. After that, the PI controller is used to reduce the mistake.Afterwards, the system stability is ensured by adding the restriction block, which limits the inaccuracy to the lowest and maximum inductance that the TCR can offer.The following equation is used by the linearization block, which is based on a lookup table, to extract the firing angle α.

ISSN: 1832-5505
Vol-7 Issue-01 FEB 2019

$$L_{FI}(\alpha) = \pi \frac{L_{FI}}{-2\alpha + \sin(2\alpha) - 2\pi}, \ \frac{\pi}{2} \le \alpha \le \pi \qquad (1)$$

Where α *FI L* is the real inductance of the TCR and (α)*FI L* is the estimated inductance that the TCR should provideusing α.Fig. 2 (b) presents the block diagram of the transfer function, which ismodeledbasedonthecontrolblockofFig.2(a).AccordingtoFig.1(b)andFig.2(b),theopen loop transfer function of the EPS is expressed as:

$$G_{CT} = \frac{V_{lo}}{V_s} = \frac{Z_{Fi}}{1 + \frac{Z_{Fi}}{Z_L}} Z \cdot (k_p + \frac{k_i}{s}) \qquad (2)$$

where the TCR's firing angle is located.The analogous FC-TCR impedance is represented as Fi Z, and LZistheloadimpedance, Zisthelineimpedance (LsZ) plus the series filter inductance lo L (assuming the series filter resistor is ignored)

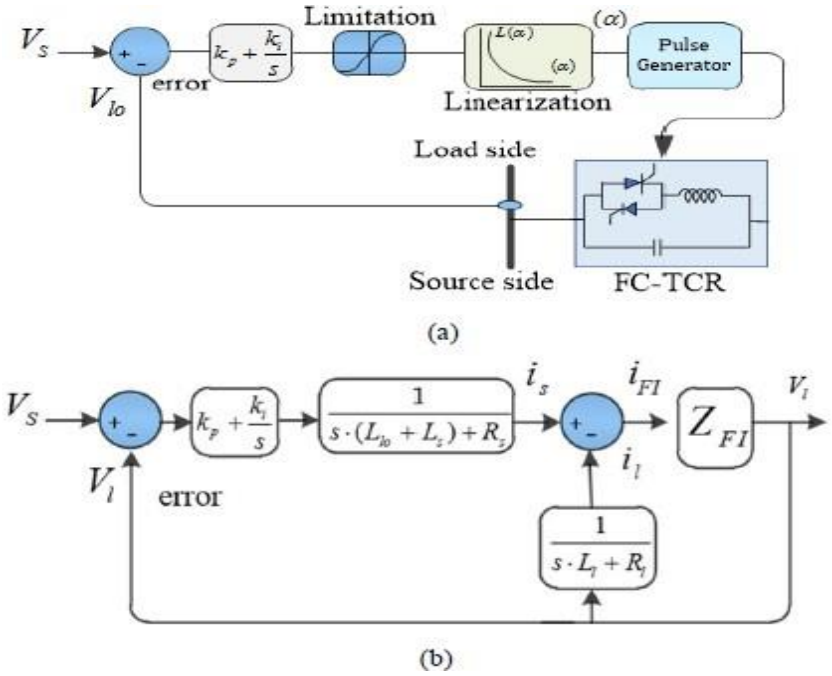

Fig.2:VoltageregulatoroftheTCR.*(a)*controlblockoftheTCR.*(b)*blockdiagramdepictsthetransfer function of *(a)*.

$$Z_{Fi} = \frac{(s \cdot L_{Fi} + R_{LFi}) \cdot (\frac{1}{s \cdot C_{Fi}} + R_{CFi})}{s \cdot L_{Fi} + R_{LFi} + \frac{1}{s \cdot C_{Fi}} + R_{CFi}} =$$

$$\frac{s^2 \cdot L_{Fi} \cdot C_{Fi} \cdot R_{CFi} + s \cdot (L_{Fi} + (R_{LFi} \cdot R_{CFi} \cdot C_{Fi})) + R_{LFi}}{s^2 \cdot L_{Fi} \cdot C_{Fi} + s \cdot C_{Fi}(R_{LFi} + R_{CFi}) + 1} \qquad (3)$$

ISSN: 1832-5505
Vol-7 Issue-01 FEB 2019

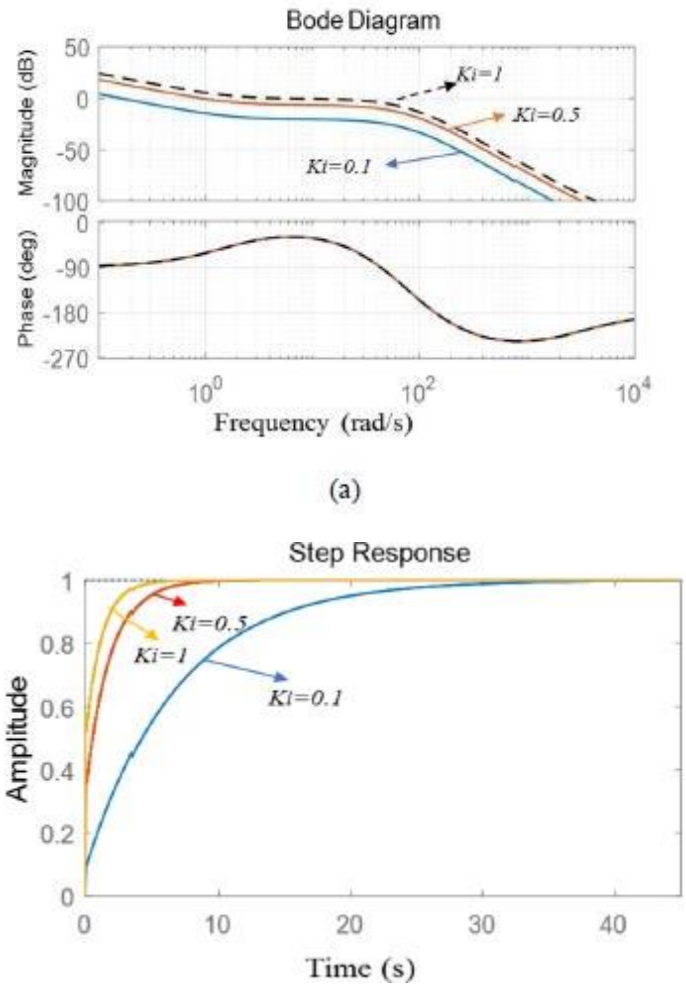

Fig.3:stabilityassessmentoftheTCR. *(a)*Bodeplotofequation(4)*(b)*Stepresponseofequation(4).

The open loop transfer function shown in (4) is the outcome of substituting (3) in (2).To obtain a stable system with a quicker reaction, the parameter of the PI controller may be designed using the open loop transfer function of equations (5).Because the transfer function is both big and of order 4, the Control System Toolbox in MATLAB may be used to tune the gains Ki and Kp. The step response of CT G and the Bode diagram are shown in Figure 3. Figure 3 shows that for a stable system with a quick reaction, a suitable phase and gain margin is Kpto 0 and Ki around 1.

A. HAPFModeling

One of the goals of the HAPF is to reduce the harmonic distortion of the EPS that is produced by non-linear loads and the transconductance resonance (TCR). The APF's reference compensating currents are generated to the switches via the MPC after being calculated using the synchronous reference frame based on the least square

ISSN: 1832-5505
Vol-7 Issue-01 FEB 2019

technique provided in [15].Faster transient response, simpler design (no extensive modelling or transfer functions of the physical system required), and resilience during parameter changes are only a few of the benefits of this latter over conventional controllers [16].The imbalance of the system is believed to be overlooked as the heavyload of the ship, the propellers, are three-phase systems that consume around 90% of the entire power of the ship.Therefore, it is believed that the harmonics produced by the variable speed drives are 6h±1, with h being the harmonic order.So, the equations for the dynamic load at the harmonic order of 6h±1 may be represented as shown in Figure 1 (b).

$$\begin{bmatrix} L_{Fi1}\dfrac{di_{s1}(t)}{dt}+c_{Fi1}\int i_{s1}(t)dt \\ L_{Fi2}\dfrac{di_{s2}(t)}{dt}+c_{Fi2}\int i_{s2}(t)dt \\ L_{Fi3}\dfrac{di_{s3}(t)}{dt}+c_{Fi3}\int i_{s3}(t)dt \end{bmatrix}=\begin{bmatrix} -V_{dc}\cdot S-R_{s1}\cdot i_{h1} \\ -V_{dc}\cdot S-R_{s2}\cdot i_{h2} \\ -V_{dc}\cdot S-R_{s3}\cdot i_{h3} \end{bmatrix} \tag{5}$$

$$\begin{bmatrix} i_1(t) \\ i_2(t) \\ i_3(t) \end{bmatrix}=\begin{bmatrix} \sum_i I_i \sin(i(wt+\Phi_{s,i})) \\ \sum_i I_i \sin(i(wt+\Phi_{s,i}-\dfrac{2\pi}{3})) \\ \sum_i I_i \sin(i(wt+\Phi_{s,i}+\dfrac{2\pi}{3})) \end{bmatrix}, \forall i \in 6h\pm 1, \quad h=1,2,\ldots,N \tag{6}$$

In order to simplify the calculation and reduce the computation burden of the MPC, the sum of theharmoniccurrentsaretransformedintoα,βstationaryframeusingClarktransformasshown in (7).

$$G_{CT}=\frac{\dfrac{s^2\cdot L_{Fi}\cdot C_{Fi}\cdot R_{CFi}+s\cdot(L_{Fi}+(R_{LFi}\cdot R_{CFi}\cdot C_{Fi}))+R_{LFi}}{s^3\cdot L\cdot L_{Fi}\cdot C_{Fi}+s^2\cdot(R_s\cdot L_{Fi}\cdot C_{Fi}+C_{Fi}\cdot L\cdot(R_{LFi}+R_{CFi}))+s\cdot(C_{Fi}\cdot R_s\cdot(R_{LFi}+R_{CFi})+L)+R_s}}{\dfrac{s^2\cdot L_{Fi}\cdot C_{Fi}\cdot R_{CFi}+s\cdot(L_{Fi}+(R_{LFi}\cdot R_{CFi}\cdot C_{Fi}))+R_{LFi}}{s^3\cdot L_l\cdot L_{Fi}\cdot C_{Fi}+s^2\cdot(R_l\cdot L_{Fi}\cdot C_{Fi}+C_{Fi}\cdot L_l\cdot(R_{LFi}+R_{CFi}))+s\cdot(C_{Fi}\cdot R_l\cdot(R_{LFi}+R_{CFi})+L_l)+R_l}+1}(k_p+\frac{k_i}{s}) \tag{4}$$

ISSN: 1832-5505
Vol-7 Issue-01 FEB 2019

$$\begin{bmatrix} i_\alpha(t) \\ i_\beta(t) \end{bmatrix} = \begin{bmatrix} \frac{2}{3} & -\frac{1}{3} & -\frac{1}{3} \\ 0 & \frac{1}{\sqrt{3}} & -\frac{1}{\sqrt{3}} \\ \frac{1}{3} & \frac{1}{3} & \frac{1}{3} \end{bmatrix} \cdot \begin{bmatrix} i_{s1}(t) \\ i_{s2}(t) \\ i_{s3}(t) \end{bmatrix} \Rightarrow i_T(k) = i_\alpha + j i_\beta \quad (7)$$

After that, the application of MPC requires the discretization of the derivatives and the integrals, this can beachieved using Euler approximation as shown in the following equations:

$$\frac{di}{dt} = \frac{i_T(k+1) - i_T(k)}{T_s} \qquad (8)$$

$$\int i dt = i(k) + T_s i(k) = i(k+1) \qquad (9)$$

Substituting(8)and(9)in(7)resultsinthefollowingequationswhichpresentthepredictionstep of each state.

$$i_T(k+1) = -SV_{dc} - i_T(k)(R_s + \frac{L_s}{T_s}) \frac{1}{\frac{L_s}{T_s} + c} \qquad (10)$$

2.0 PRcontroller

In order to achieve infinite gain at the AC frequency of ϋ0 and force the steady-state voltage error to zero, the ideal resonant controller can be mathematically derived by transforming an ideal synchronous frame PI controller to the stationary frame. At other frequencies, there is no phaseshift and gain is nonexistent. Its tuning for Kp is same to that of a PIcontroller. It is challenging to implement the PR controller in practice because the ideal PR controller behaves like a network with an unlimited quality factor.To begin, neither an analogue nor a digital system can reach the infinite quality factor that results from the infinite gain imposed by the PR controller. Secondly, the PR controller's gain is much lower at frequencies outside of the grid voltage's harmonic impact, and it is insufficient to eradicate this effect. Hence, a PR controller that is approximately optimal but not perfect.

ISSN: 1832-5505
Vol-7 Issue-01 FEB 2019

$$G_S(s) = K_p + \frac{2K_i s}{s^2 + \omega_0^2}$$

$$G_S(s) = K_p + \frac{2K_i \omega_{cut} s}{s^2 + 2\omega_{cut} s + \omega_0^2}$$

the grid frequency is ω0(=2π×60rad/s) and the cutoff frequency is ωcut, where Kp and Kia are constants.

There is less sensitivity of the controller to fluctuations in light grid frequencies, and a broader bandwidth is shown around the resonant frequency.Even though it isn't a perfect PR controller, the non-ideal one responds similarly at various harmonic frequencies. It is evident from the equation that the PR controller has three parameters, namely Kp, Ki, and

then cut. To make things easier to understand, we'll pretend that two of these factors are fixed so that we can see how changing the third one affects the results.

Method A.SVPWM

The d, q plane, which represents voltages as space vectors, is the basis of an alternative method to SPWM. The Park transform is used to find the d and q components while keeping the overall power and impedance constant.

The phase-to-centre voltage, V*, is derived by properly selecting nearby vectors V1 and V2, and eight space vectors are shown in Fig. 4 according to the inverter switching locations.

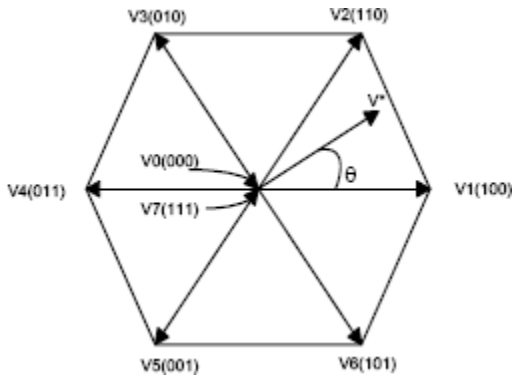

Fig.4 Inverteroutputvoltagespacevector

Thereferencespace vectorV* is givenby Equation (1), whereT1, T2 are theintervals of application of vector V1 and V2 respectively, and zero vectors V0 and V7 are selected for T0.

V* Tz=V1*T1 +V2 *T2 +V0 *(T0/2)+V7 *(T0/2)

Fig. below shows that the inverter switching state for the period T1 for vector V1 and for

ISSN: 1832-5505
Vol-7 Issue-01 FEB 2019

vectorV2,resultingswitchingpatternsofeachphaseofinverterareshowninFig.pulsepatternof space vector PWM.

Applied GIS

ISSN: 1832-5505

Vol-7 Issue-01 FEB 2019

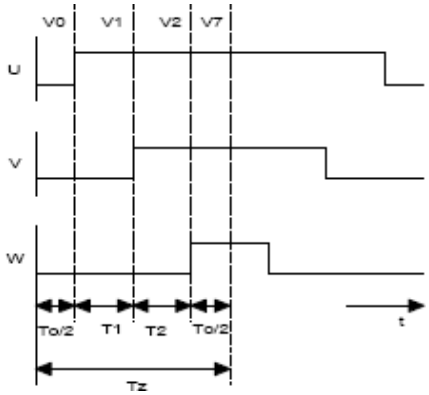

Fig.5 PulsepatternofSpacevectorPWM

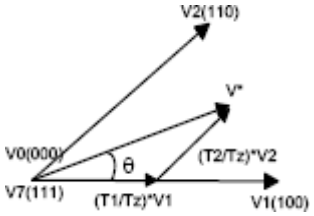

Fig.6 DeterminationofSwitchingtimes

In order to apply three-phase system voltages to the controlled output, the Pulse Width modulation method may be used. The idea behind Space Vector Modulation (SVM) is different from conventional pulse width modulation (PWM) procedures as it generates all three inverter drive signals at the same time.Less operation time and programme memory are required for the implementation of SVM processes in digital systems. The PWM waveforms are shown in Figures 5 and 6.

3.0 Simulation results

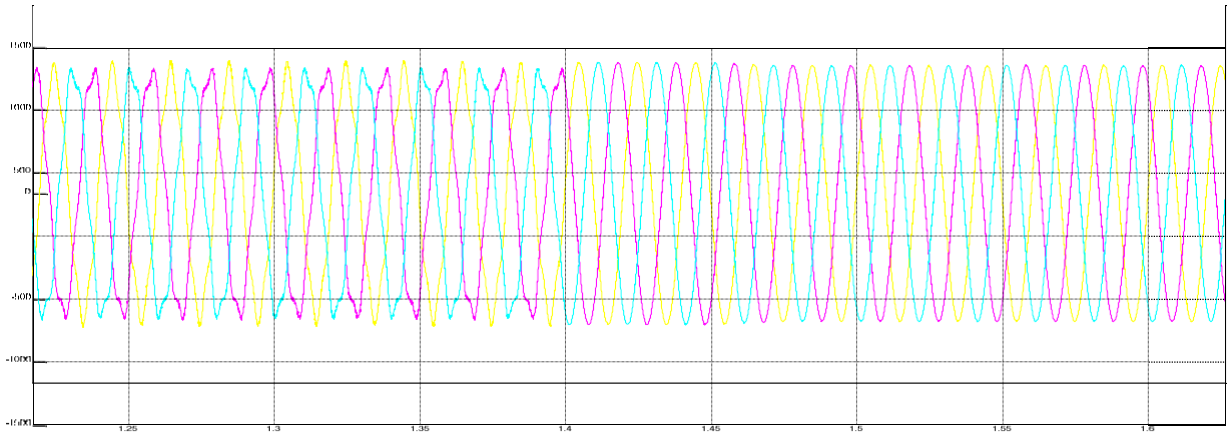

Fig.7 VoltageVol

ISSN: 1832-5505
Vol-7 Issue-01 FEB 2019

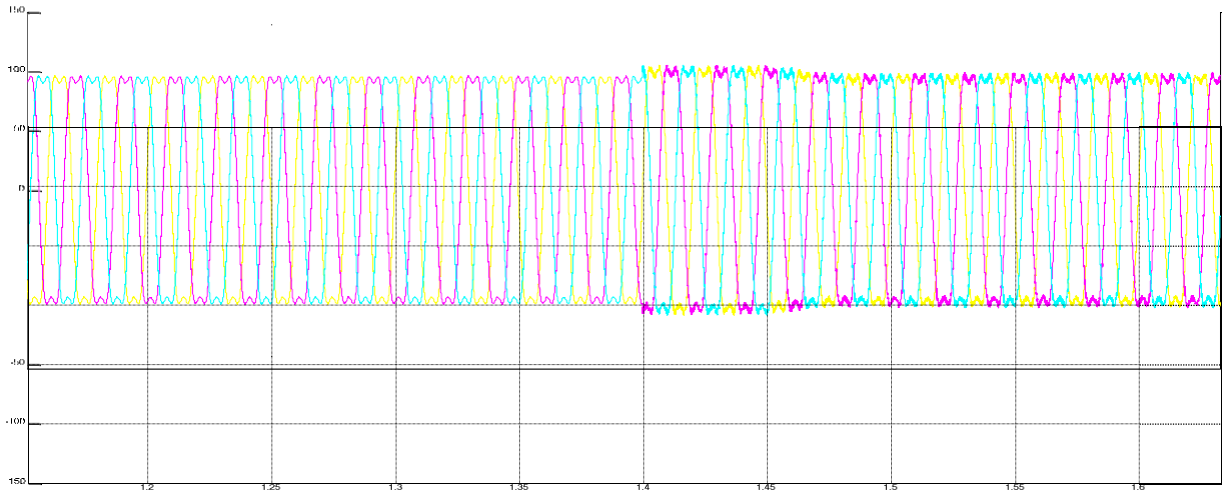

Fig.8 Load Current

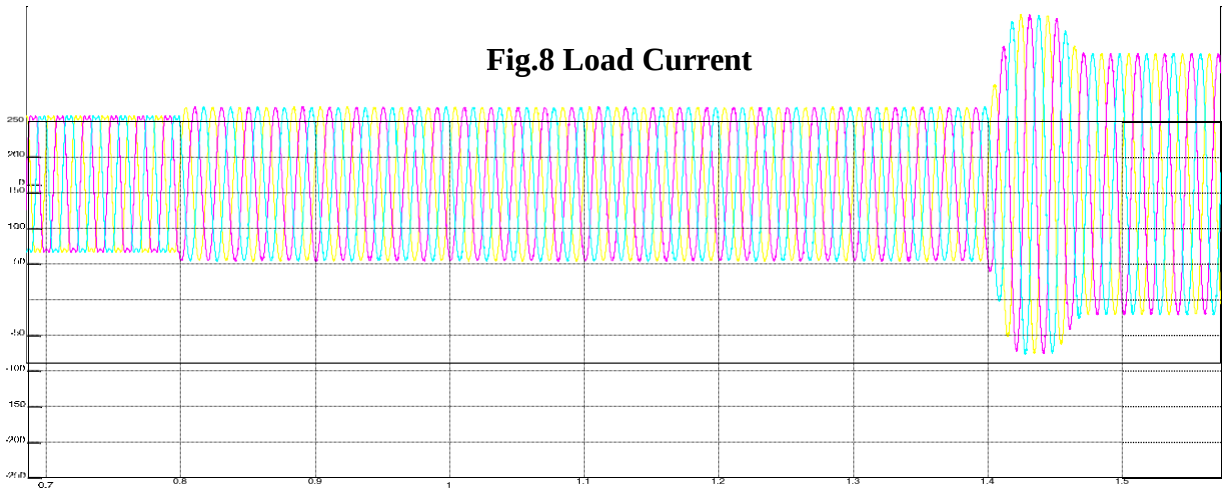

Fig.9Source Current

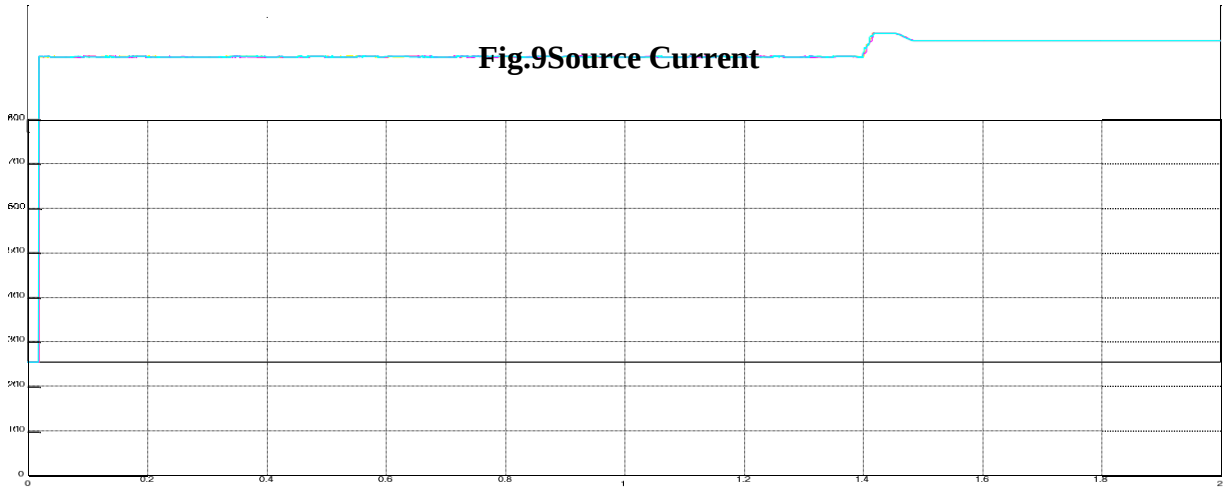

Fig.10 Voltage Magnitude

ISSN: 1832-5505
Vol-7 Issue-01 FEB 2019

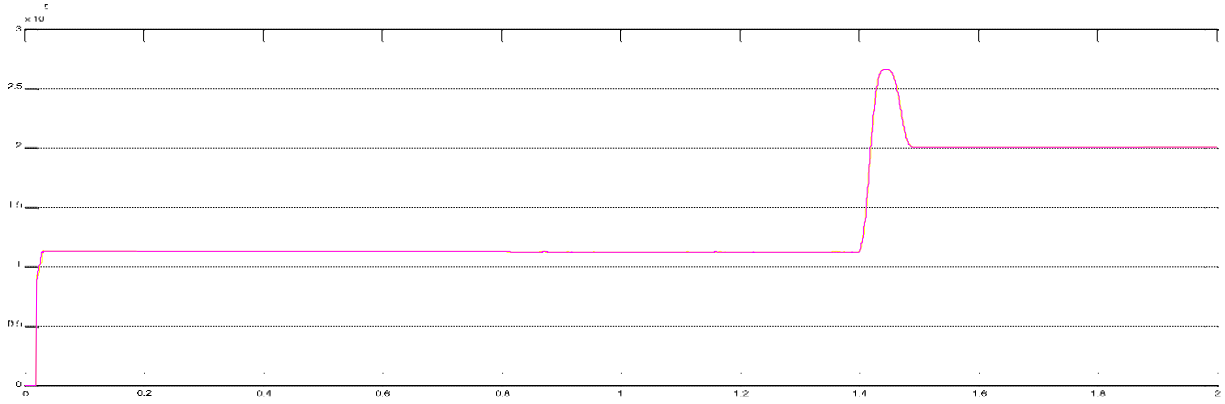

Fig.11ActivePower

4.0 Conclusion

This research proposes a hybrid structure that combines HAPE and FC-TCR with a PR-SVPWM method to correct for voltage and sag fluctuations. In order to reduce harmonic oscillations in the suggested system, the devised HAPE is used. In addition, the PR-based SVPWM method improves system stability more effectively. The MATLAB/Simulink environment was used for the system's design. The simulation results show that the suggested PR-based SVPWM effectively reduces harmonics at unknown frequencies

.

.

References

[1] "ABSGuidanceNotesonControlofHarmonicsinElectricalPowerSystems,AmericanBureau of Shipping, Huston, USA, 2006."

[2] S. Jayasinghe, L. Meegahapola, N. Fernando, Z. Jin, and J. Guerrero,"Review of Ship Microgrids:SystemArchitectures,StorageTechnologiesandPowerQualityAspects,"Inventions, vol. 2, no. 1, p.4, 2017.

[3] G. Sulligoi, A. Vicenzutti, V. Arcidiacono, and Y. Khersonsky,"Voltage Stability in Large Marine Integrated Electrical and ElectronicPower Systems," IEEE Trans. Ind. Appl., vol. 9994, no. c, pp. 1–1,2016.

[4] J.Mindykowski,"Powerqualityonships:Todayandtomorrow'schallenges,"EPE2014-Proc. 2014 Int. Conf. Expo. Electr. PowerEng., no. December 2014, pp. 1–18, 2014.

ISSN: 1832-5505
Vol-7 Issue-01 FEB 2019

[5] R.E.Hebneretal.,"Technicalcross-fertilizationbetweenterrestrialmicrogridsandshippower systems," J. Mod. Power Syst. CleanEnergy, vol. 4, no. 2, pp. 161–179, 2016.

[6] Y. Terriche, D. Kerdoun, and H. Djeghloud, "A new passivecompensation technique to economically improve the power quality oftwo identical single-phase feeders," 2015 IEEE 15th Int. Conf.Environ. Electr. Eng. EEEIC 2015 - Conf. Proc., no. 2, pp. 54–59,2015.

[7] R.M. S. Q.Mary, "RMS QueenMary 2 ReportNo 28/2011.," no. 28,2011.

[8] Y. Terriche, S. Golestan, J. M. Guerrero, D. Kerdoune, and J. C.Vasquez, "Matrix pencil method-based reference current generation forshunt active power filters," IET Power Electron., vol. 11, no. 4, 2018.

[9] J.Mindykowski,"CaseStudy—BasedOverviewofSomeContemporaryChallengestoPower Quality in Ship Systems,"Inventions, vol. 1, no. 4, p. 12, 2016.

[10] T.Demirdelen,M.Inci,K.C.Bayindir,andM.Tumay,"Reviewofhybridactivepowerfilter topologies and controllers," in 4thInternational Conference on Power Engineering, Energy andElectrical Drives, 2013, pp. 587–592.

[11] P.P.Biswas,P.N.Suganthan,andG.A.J. Amaratunga,"Minimizingharmonicdistortionin powersystemwithoptimaldesignofhybridactivepowerfilterusingdifferentialevolution,"Appl. Soft Comput. J.,vol. 61, pp. 486–496, 2017.

[12] S.Rahmani,A.Hamadi,K.Al-Haddad,andL.A.Dessaint,"ACombinationof ShuntHybrid PowerFilterandThyristor-ControlledReactorforPowerQuality,"IEEE Trans.Ind.Electron.,vol. 61, no. 5,pp. 2152–2164, May 2014.

[13] L.Wang,"HybridStructureofStaticVarCompensatorandHybridActivePowerFilter(SVC //HAPF)forMedium-VoltageHeavyLoadsCompensation,"vol.65,no.6,pp.4432–4442,2018.

[14] First, Ed., Van Cutsem, Thierry, and Costas Vournas. Voltage stabilityof electric power systems. Springer Science & Business Media, 2007.

[15] Y. Terriche, J. M. Guerrero, and J. C. Vasquez, "Performanceimprovement of shunt active powerfilterbasedonnon-linearleastsquareapproach,"Electr.PowerSyst.Res.,vol.160,pp.44– 55, Jul.2018.

[16] J.RodriguezandP.Cortes, Predictivecontrolofpowerconvertersandelectricaldrives.John Wiley & Sons, 2012.